Defect and Diffusion Forum
ISSN: 1662-9507, Vol. 451, pp 157-167
doi:10.4028/p-rD7QdB

Submitted: 2026-01-30
Revised: 2026-02-25
Accepted: 2026-03-01
Online: 2026-04-17

Thermal Transient Modelling and Experimental Validation of Hybrid Polymer-Steel Moulds for Micro-Injection Moulding

Giulia Zaniboni[1,a*], Vito Basile[2,b], Riccardo Pelaccia[1,c], Rossella Surace[2,d], Keltoum Oubellaouch[3,e], Francesco Modica[2,f], Leonardo Orazi[1,3,g], Giovanna Rotella[4,h], Luigino Filice[5,i], Irene Fassi[6,j]

[1]University of Modena and Reggio Emilia, DISMI, Via Amendola 2, 42122, Reggio Emilia, Italy

[2]CNR-STIIMA, National Research Council, Via P. Lembo 38 F, 70124 Bari, Italy

[3]University of Modena and Reggio Emilia, EN&TECH, Piazzale Europa 1, 42124, Reggio Emilia, Italy

[4]University LUM G. Degennaro, Dept. of Engineering, S.S. 100 Km 18, Casamassima, 70010, Italy

[5]University of Calabria, DIMEG, cube 45C, Ponte P.Bucci, 87036 Rende, Italy

[6]CNR-STIIMA, National Research Council, Via A. Corti 12, 70124 Bari, Italy

[a*]giulia.zaniboni@unimore.it*, [b]vito.basile@stiima.cnr.it, [c]riccardo.pelaccia@unimore.it, [d]rossella.surace@stiima.cnr.it, [e]keltoum.oubellaouch@unimore.it, [f]francesco.modica@stiima.cnr.it, [g]leonardo.orazi@unimore.it, [h]rotella@lum.it, [i]luigino.filice@unical.it, [j]irene.fassi@stiima.cnr.it

Keywords: thermal management, hybrid moulds, injection moulding, additive manufacturing.

Abstract. Efficient thermal management is a key factor in improving the sustainability and productivity of injection moulding processes, particularly at the micro-scale where thermal transients strongly affect part quality and cycle stability. This work investigates the thermal behaviour of hybrid moulds composed of polymeric support plates manufactured in Precision Resin V01 and stainless-steel inserts manufactured by additive manufacturing. An experimental campaign was carried out on a micro-injection moulding machine to characterize the intrinsic thermal response of the mould under uncooled conditions. Temperatures were monitored through embedded thermocouples and used to develop and calibrate a three-dimensional transient numerical model in COMSOL Multiphysics. Particular attention was devoted to the identification and calibration of heat transfer coefficients at the injection and extraction interfaces, which were found to play a dominant role in governing insert temperature evolution. The calibrated model accurately reproduces the experimental thermal transients, with deviations below 10%, demonstrating its reliability as a predictive tool for analysing mould thermal behaviour and supporting early-stage design and process optimization. The results highlight the advantages of hybrid architectures in promoting thermal stability and provide a robust methodology for modelling heat exchange in unconventional mould configurations.

Introduction

Injection moulding is a widely adopted manufacturing process to produce high-volume plastic components, owing to its versatility in processing a broad range of materials and its capability to produce complex geometries with high precision [1]. Given the dominant role of injection moulding in the plastics industry, its energy performance has become a key factor in sustainability assessments [2]. Among the different stages of the process, thermal energy management plays a critical role, as it directly influences process efficiency, part quality, and overall cost-effectiveness. In particular, cooling time is one of the most influential parameters affecting cycle time and energy consumption; its optimization can therefore result in significant energy savings [3]. Therefore, improving thermal management within the mould represents a crucial strategy for reducing the environmental footprint of injection moulding processes [4]. The thermal behaviour of the mould is strongly affected by the thermal conductivity of the materials used in its construction. Traditionally, moulds and inserts are manufactured from high-strength steels because of their excellent mechanical resistance and favourable thermal properties. However, steel moulds are associated with high material and manufacturing costs, as well as long production and maintenance lead times [5]. Conversely, in application fields where extreme mechanical loads are not required, the use of polymeric materials for mould fabrication can significantly reduce both cost and weight. Moreover, the inherently low thermal conductivity of polymers can be exploited to thermally insulate the mould cavities, promoting a more stable thermal field during processing. Nevertheless, previous studies investigating moulds entirely manufactured from polymeric materials have reported limited service life and reduced part quality, highlighting the mechanical limitations of fully polymeric mould configurations [6-8].

Building upon these findings, a hybrid mould concept can be proposed, combining steel inserts with polymeric or composite mould base components, such as support plates. This hybrid architecture mitigates mechanical weaknesses by retaining steel in critical regions while exploiting the advantages of polymers and composites, including lightweight design and thermal insulation capabilities. Such an approach enables improved thermal stability without compromising structural integrity or mould durability. In parallel, the rapid development of additive manufacturing (AM) technologies has expanded both material and geometric design possibilities for mould systems, enabling innovative architectures and enhanced thermal control strategies [9]. Beyond material flexibility, AM allows the fabrication of complex geometries that are not achievable with conventional manufacturing techniques, such as conformal cooling channels that closely follow the geometry of the moulded cavity. These channels enable localized and more uniform heat removal, leading to improved temperature control and reduced cycle times [10,11]. Current research frequently investigates mould inserts or plates produced via AM using polymeric or composite materials, while maintaining conventional steel moulds to ensure mechanical robustness [6,7]. Retaining a steel mould core with AM-fabricated cavities therefore allows the benefits of conformal cooling to be realized without the limitations associated with fully polymeric moulds.

At the same time, the introduction of polymeric or composite mould base components significantly alters the thermal behaviour of the system. Acting as thermal insulators rather than heat conductors, these components promote faster temperature stabilization of the steel inserts and improved robustness during extended mould-opening intervals. Furthermore, since the polymeric elements do not directly contain the mould cavities, mechanical stresses are reduced, overcoming the durability limitations of fully polymeric moulds and making the hybrid approach competitive also in terms of service life. The use of lightweight polymeric components additionally reduces the mechanical energy required for mould movement during production cycles and mould-change operations. From a broader perspective, this innovative mould design contributes to the development of a more sustainable injection moulding process.

Despite these advantages, precise thermal control remains essential to prevent the mould from drifting into thermal instability. While the low thermal conductivity of polymeric mould components can be advantageous for heat accumulation during the injection phase, it may hinder the recovery of thermal stability during cooling.

In the specific case of micro-injection moulding, thermal management becomes even more critical because of the small characteristic dimensions of the cavity and the resulting high surface-to-volume ratio of the moulded parts. Compared to conventional injection moulding, heat is extracted much more rapidly through the mould walls, promoting the early formation of a frozen layer that restricts flow and hinders the complete replication of high-aspect-ratio micro-features. Consequently, mould temperature during filling has been identified as one of the most influential parameters governing cavity filling, replication accuracy and part quality. Several studies have therefore proposed dynamic or rapid thermal control strategies, such as variotherm systems or rapid surface heating approaches, to locally increase mould temperature during the filling stage and delay premature solidification [12-15]. More generally, micro-injection moulding cannot be regarded as a simple downscaling of the conventional process, since the reduced dimensions amplify heat-transfer effects and make the process strongly dependent on boundary conditions at the polymer–mould interface [16]. In this context, an accurate description and calibration of the heat transfer coefficients at the injection and extraction sides becomes essential for the reliable prediction of mould thermal transients and for the correct design of thermally optimized tooling solutions.

Within this framework, the present research aims to evaluate a novel hybrid mould design employing unconventional materials to optimize thermal energy utilization in micro-injection moulding. An experimental campaign was conducted to characterize the intrinsic thermal behaviour of the mould under uncooled operating conditions. A transient finite-element model was developed in COMSOL Multiphysics as it is a well-established tool for simulating complex multiphysics phenomena and heat transfer in injection moulding processes [17]. The numerical model was then calibrated using experimental measurements.

Particular emphasis was placed on the identification of boundary conditions and on the calibration of heat transfer coefficients at the interfaces with the injection and extraction systems, which significantly influence the thermal response of small-scale inserts. The validated numerical model is proposed as a reliable tool to support mould design and to predict thermal stability, reducing the need for time-consuming trial-and-error experimental procedures.

Experimental Setup

Design and manufacturing of the hybrid mould.

The mould for micro-injection moulding was designed according to previous investigations [18]. The mould has a multi-material structure and was manufactured with Additive Manufacturing (AM) technologies. The design of the mould inserts is optimized in terms of material, mechanical and thermal performance, with conformal cooling realized with channels having a 3D-evolution all around the mould cavity. They are made of bulk stainless steel to resist to high injection and holding pressures and to promote the heat extraction from the cavity [18]. Support plates should guarantee mechanical performance and thermal insulation of the mould core inserts. The former objectives are the mechanical properties, such as stiffness and toughness, that are required to obtain efficient guiding and couplings between the injection (fixed) and ejection (mobile) sides of the mould while closing/opening phases and the mating on the parting surface. This objective is achieved selecting suitable materials, using high accuracy manufacturing technologies and guiding/coupling components, such as columns and bushes. The latter requirement is thermal insulation, which is obtained by using polymeric materials. Furthermore, the design of the support plates was topologically optimized with mixed bulk-lattice structures [19]. The outcomes of the design task are 3D solid models developed with the 3D CAD Solidworks release 2023 SP 5.0. The mould micro-cavity (Figure 1) was conceived with a complex 3D shape having curved thin walls and variable thicknesses, thus requiring a 3D evolution of conformal cooling channels and exploiting all potentialities of AM technologies.

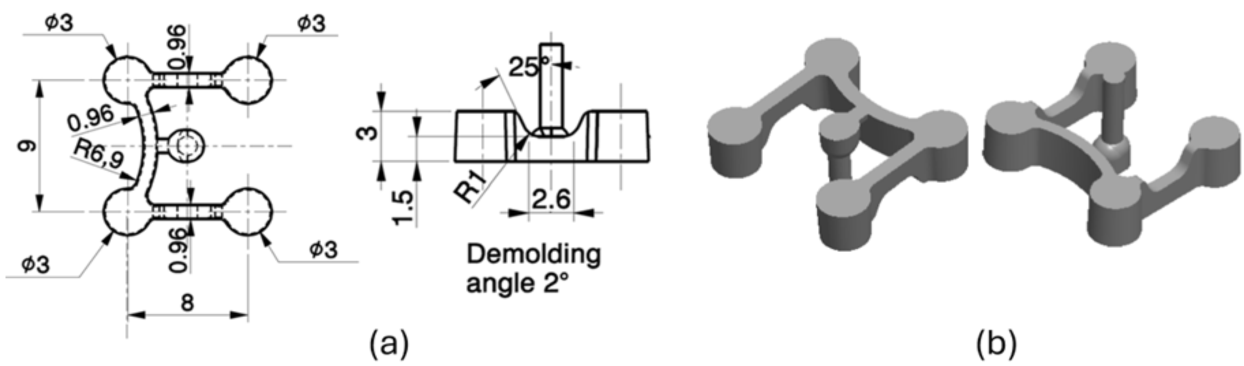

Fig. 1. Drawing (a) and 3D views (b) of the moulding part.

The mould inserts were fabricated using a Markforged MetalX, which implements a Metal-Extrusion (MEX) AM technology, and a 17-4PH stainless steel. Holes, mating and coupling surfaces were finished by CNC milling on a CMX1100V DMG Mori machine, while the cavity was finished using a Micro-Electrical Discharge Machine (μ-EDM) Sarix SX200 machine. The support plates were realized by stereolithography (SLA) using a Formlabs Form4 machine and a photopolymer resin

Formlabs Precision Model V01 (FLPMBE01). Parts were printed on the build platform setting a layer thickness of 25µm. After processing, parts were washed for 10 minutes with Tripropylene Glycol Monomethyl Ether (TPM) solvent with a Formlabs Wash 2nd-Gen machine and UV-cured for 35 minutes at 35°C with a Formlabs Cure V1 machine. Mould inserts design is presented in Figure 2.

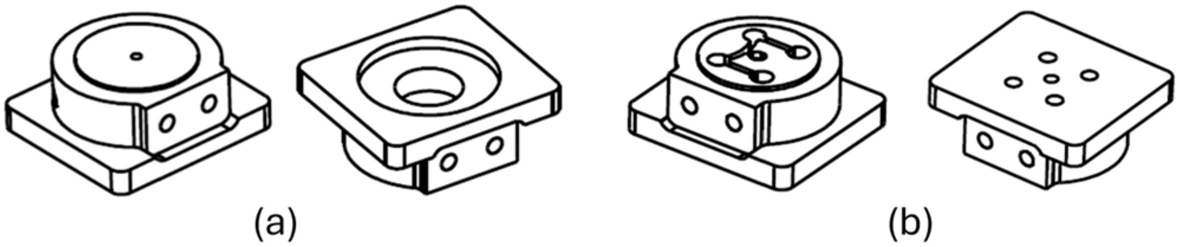

Fig. 2. Drawing of the moulding part. Injection side (a) ejection side (b).

Experimental setup of injection moulding process without cooling.

To perform experimental tests, a DesmaTec Formica Plast 1K injection moulding machine was used. The machine can have a maximum injected volume of 150 mm^3, a maximum injection pressure of 300 MPa, and a maximum injection rate of 3.5 cm^3/s. The injection moulding material was a Polyoxymethylene (POM) BASF Ultraform N2320 003. To ensure a correct evaluation of polymer effect on insert temperatures, during the cooling step no coolant circulation was adopted. Therefore, the cooling was obtained by heat transmission with the mould kept below the glass transition temperature, but defined by the injection moulding thermal transient starting from the ambient temperature of about 15°C.

The thermal monitoring system consisted of four K-type thermocouples connected to MAX6675 digital modules interfaced with an Arduino Uno platform. Thermocouples T1 and T4 were embedded within the ejection and injection inserts, respectively, through precision holes positioned in close proximity to the mould cavity (Figure 3). Thermocouples T2 and T3 were mounted on the external surfaces of the support plates on the injection and ejection sides, respectively (Figure 3). This monitoring configuration enabled a detailed analysis of the thermal transients over the 80-cycle experimental campaign (Figure 4). Notably, no active cooling was applied, allowing the investigation of the intrinsic thermal behaviour of the polymer moulds. The transient thermal evolution began with the tooling set at room temperature (15 °C). Two repetitions of the same experimental trial were conducted to evaluate the repeatability of the thermal response. The process parameters adopted for the experimental tests are reported in Table 1.

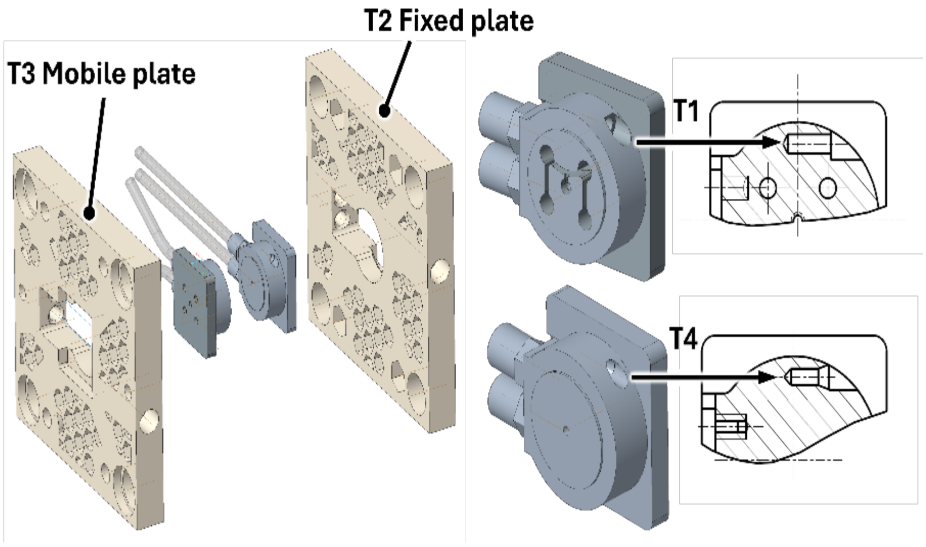

Fig. 3. Thermocouple locations on plates and inserts.

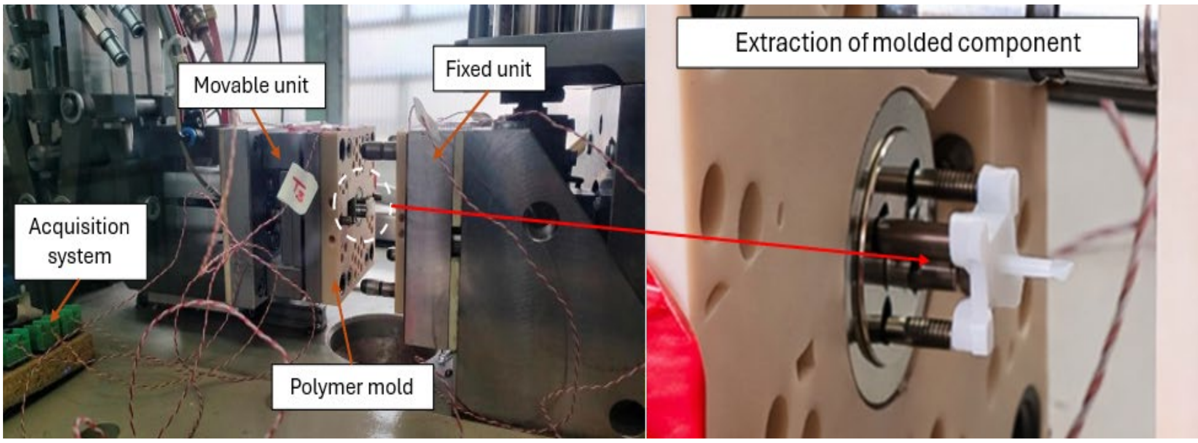

Fig. 4. Experimental configuration for testing the final mould setup.

Table 1. Injection moulding process parameters in experimental test.

Process parameters/Event	Symbol	Units	Value/Detail
Melt Temperature	*Tmelt*	°C	230
Initial mould temperature	*Tmould*	°C	15
Filling time	*tfill*	s	0,25
Holding time	*thold*	s	4
Cooling time (no coolant)	*tcool*	s	4
Mould open/close time	*topen*	s	3
Cycle time	*tcycle*	s	11,25
Total Number of cycles	*n*	s	80

Experimental setup for thermal boundary condition calibration.

To calibrate the heat transfer coefficients (HTCs) at the injection and extraction interfaces, a preliminary experimental test was conducted under closed-mould conditions, with the injector positioned in contact with the fixed insert but without polymer injection. This configuration allowed the thermal interaction between the machine units and the mould to be isolated from the effects of the molten polymer. The mould assembly was subjected to a controlled heating phase lasting approximately 500 s, during which the temperature evolution of the inserts was continuously monitored using thermocouples embedded in the fixed and movable inserts (T4 and T1, respectively). The injector temperature was set to 230 °C, corresponding to the melt temperature adopted during the subsequent POM moulding trials. This approach enabled a targeted characterization of the heating contribution provided by the hot injector in contact with the fixed side, as well as the thermal inertia of the extraction unit, which tends to maintain the movable side at lower temperatures. In micro-injection moulding, thermal transients are strongly influenced by heat exchange with the surrounding machine components, owing to the reduced mass and limited thermal inertia of the inserts. Consequently, an accurate calibration of the HTCs at these interfaces is essential for correctly reproducing the measured temperature evolution and for ensuring the predictive capability of the numerical model.

Numerical Model of the Process

In the numerical model, the original geometry was simplified by modelling the injection and extraction units as equivalent plates with comparable heat exchange characteristics (Figure 5), while auxiliary features such as bolt holes were removed. These geometry simplifications reduced meshing complexity and significantly decreased computational costs without compromising model accuracy. The simulations employed the Heat Transfer in Solids module to solve transient heat conduction within the mould assembly, including convective heat losses at the external boundaries.

The numerical analysis was performed using COMSOL Multiphysics 6.1, adopting a multi-physics modelling approach. A high-fidelity three-dimensional mesh comprising 482785 tetrahedral elements was generated, with a size-dependent distribution. In particular, the cavity and insert regions were discretized using a maximum element size of 1 mm to accurately capture steep thermal gradients, whereas support plates and secondary components were meshed with a maximum element size of 5 mm.

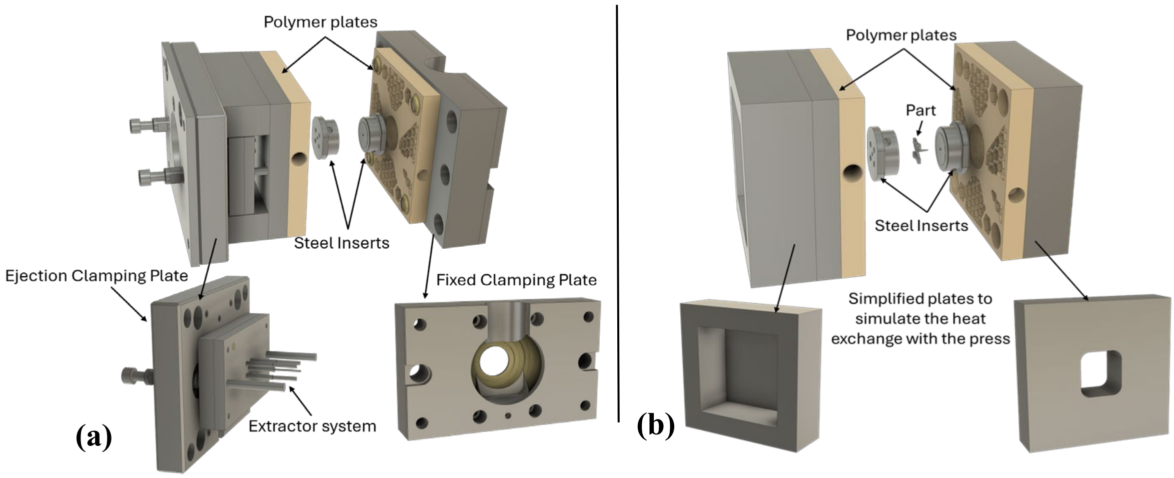

Fig. 5. (a) 3D model of the real mould block with polymer plates, (b) COMSOL Multiphysics model of polymer plates with simplified clamping plates.

The injection phase was simplified by applying a time-dependent heat source on the cavity walls, representing the thermal energy input from the molten POM at 230 °C. The temporal sequence of the process was controlled using the Events Interface Module, reproducing the experimental cycle, including filling, holding, cooling without water, and mould opening and closing phases.

Table 2 summarizes the process parameters adopted in the numerical simulations, while Table 3 reports the thermal properties of the materials implemented in the model.

As indicated in Table 2, in addition to natural heat exchange with the surrounding air, thermal interactions with the injector and extractor blocks were also accounted for. The corresponding heat transfer coefficients were identified through a dedicated calibration procedure based on the preliminary experiments performed with the mould closed and without polymer injection, as described above. The selection of the calibrated values reported in Table 2 is discussed in detail in the section *Calibration of thermal boundary conditions*.

Table 2. Process parameters and boundary conditions set within the numerical model.

Process parameters	Units	Value
Melt temperature	°C	230
Filling time	s	0.25
Holding time	s	4
Cooling time within the mould (no coolant)	s	4
Mould open/close time	s	3
Initial plates/inserts temperature	°C	15
Air (ambient) temperature	°C	15
Injector temperature	°C	230
Extractor temperature	°C	15
Heat transfer coefficient with air	$W/(m^2*K)$	15
Heat transfer coefficient with injector	$W/(m^2*K)$	600 (filling + holding), 50 (cooling)
Heat transfer coefficient with extractor	$W/(m^2*K)$	Linear decrease from 3000 to 500 in 1000s

Table 3. Material properties implemented within the numerical model.

Material Properties	Units	POM	40CrMnMo7 Stainless steel	Precision Model V01
Density	g/cm^3	1.16	7.8	1.11
Thermal conductivity	W/(m*K)	0.14	20	0.28
Heat capacity at constant pressure	J/(kg*K)	f(T), 2137 at 230 °C	500	2160

Experimental-Numerical Comparison for Model Validation

Calibration of thermal boundary conditions.

For the calibration of the heat transfer coefficients, several numerical simulations were carried out, starting from literature values. This section reports the most representative results used to justify the parameter selection summarized in Table 2. The boundary temperatures were set to 230 °C on the injection side, corresponding to the melt temperature adopted during the moulding trials, and to 15 °C on the extraction side, consistently with the initial cold-mould condition. Figure 6 presents the numerical–experimental comparison of the thermal transient obtained during the closed-mould test. Numerical results are shown for three HTC levels at the injection side (500, 600, and 750 W/m^{2}K) and two levels at the extraction side (3000 and 500 W/m^{2}K), resulting in six simulated configurations.

Considering the fixed insert (thermocouple T4), all simulations exhibit a higher initial thermal gradient than the experimental measurements, leading to a systematic overestimation of the temperature during the first 100 s. Subsequently, while the experimental curve continues to increase, the numerical predictions rapidly approach a quasi-steady regime, with a limited temperature rise (approximately 5 - 10 °C over 350 s). As a consequence, at the end of the test the measured temperature exceeds the numerical predictions, with discrepancies depending on the selected HTC combination. The smallest deviation (below 2%) is obtained for an injection-side HTC of 750 W/m^{2}K and an extraction-side HTC of 500 W/m^{2}K, whereas the largest error (about 20%) occurs for the 500-3000 W/m^{2}K configuration.

Sensitivity analysis indicates that the injection-side boundary condition has a dominant influence on the temperature evolution at T4. For a fixed injection-side HTC, variations of the extraction-side HTC produce only minor changes. This behaviour is consistent with the large temperature difference imposed at the two interfaces (230 °C versus 15 °C), which enhances the thermal driving force at the injection side.

A similar trend is observed at T1 (movable insert). Higher injection-side HTC values produce steeper initial gradients compared to the experimental data. However, while the measured temperature progressively increases due to the gradual heating of the extraction assembly, the numerical model rapidly reaches a steady condition, since constant HTC and boundary temperatures are imposed. Also in this case, the lowest final error (below 2%) is obtained for the 750–500 W/m^{2}K combination.

Based on these results, an injection-side HTC of 600 W/m^{2}K was selected as a compromise solution, ensuring deviations within approximately 10% over most of the transient. Although the 750 W/m^{2}K value minimizes the final error, it leads to larger discrepancies during the early heating stage. Furthermore, during actual moulding operations the injector is not continuously in contact with the mould, as it retracts during the cooling phases. For this reason, as reported in Table 2, the injection-side HTC is set to 600 W/m^{2}K during the active stages (filling and holding) and reduced to 50 W/m^{2}K during the passive phases. Concerning the extraction side, a time-dependent boundary condition was adopted. The HTC was assumed to decrease linearly from 3000 W/m^{2}K under cold-mould conditions to 500 W/m^{2}K, in order to limit the initial thermal gradient while progressively reducing the thermal inertia and better reproducing the gradual heating of the extraction unit.

The characteristic decay time was set to 1000 s, accounting for the intermittent injector contact and the additional cooling associated with mould opening and closing, which are expected to slow down the overall temperature rise during real processing conditions.

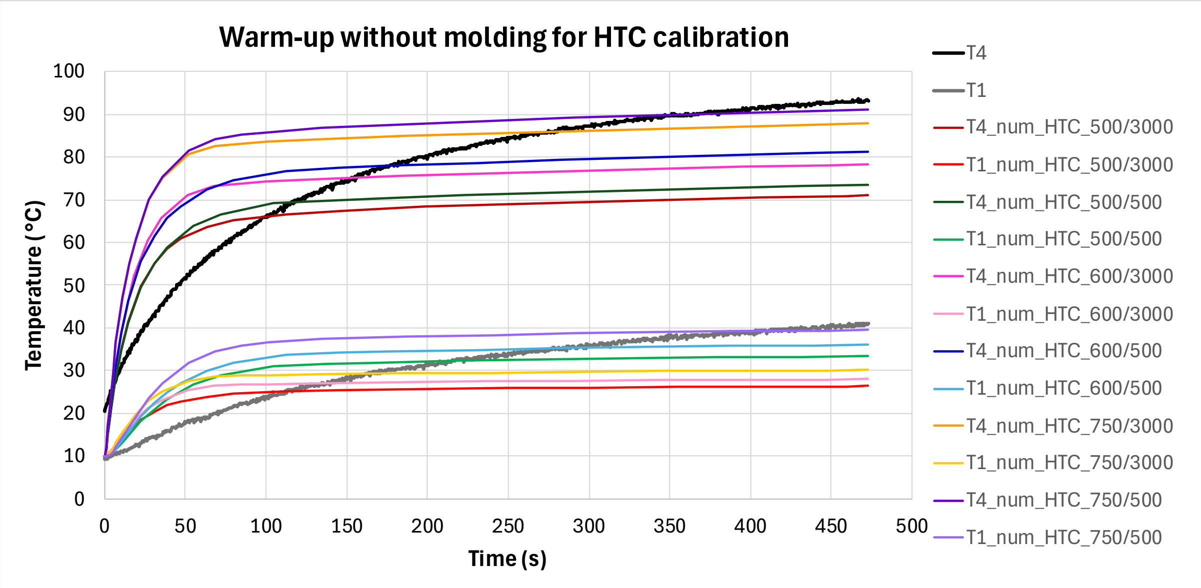

Fig. 6. Experimental–numerical comparison of temperature transients measured by thermocouples during the warm-up without moulding.

Validation of the numerical model.

The polymer moulds withstood the entire experimental campaign without exhibiting any visible damage or performance degradation, thereby confirming their mechanical reliability and structural robustness. The experimental results of the thermal field evolution recorded by the thermocouples, together with the corresponding numerical predictions, are reported in Figure 7. From the experimental data, an excellent repeatability of the measurements can be observed, as the temperature profiles obtained from the two repeated trials are nearly superimposed. This represents a significant outcome, confirming the reliability of the presented results.

A detailed analysis of the thermal transient highlights a rapid temperature increase in the fixed insert, which rises from the initial 15 °C to approximately 60 °C after 100 s of testing (corresponding to about 10 moulding cycles). Subsequently, the temperature continues to increase at a slower rate, reaching a quasi-steady condition at around 75 °C between 600 s and 900 s of operation. In contrast, both the thermal gradient and the peak temperature recorded in the movable insert are considerably lower, with a maximum value of approximately 47 °C at the end of the test. The temperature discrepancy between the fixed and movable inserts can be attributed to their respective proximity to the injection system and the ejection unit. Specifically, the injection system, which delivers the molten polymer, operates at significantly higher temperatures, whereas the extraction components are comparatively cooler. Furthermore, due to the small size of the inserts, their thermal response is strongly influenced by the thermal inertia of the surrounding press components, which may further amplify these temperature differences.

The numerical model accurately reproduces the thermal gradient trends observed experimentally in both the fixed and movable inserts. In the fixed insert, the model successfully captures both the rapid initial temperature increase and the subsequent stabilization toward a quasi-steady-state condition. Consistently with the experimental results, the numerical predictions yield a temperature of approximately 60 °C at T4 after 100 s and about 75 °C at the end of the process. However, during the thermal evolution between 100 s and 900 s, the numerical model slightly underestimates the temperature by approximately 4-5 °C, with the maximum temperature peak occurring about 100 s later than in the experimental measurements. A similar trend is observed for the movable insert, where the maximum numerical deviation reaches approximately -7 °C.

These discrepancies are most likely attributable to the definition of the boundary conditions at the injection and ejection interfaces, which strongly affect the thermal gradients of such small-scale inserts. Nevertheless, considering the complexity of the injection moulding process and the inherent simplifications adopted in the numerical model, the overall agreement can be regarded as high and fully satisfactory for the intended purpose of using the model to identify process parameters that optimize the thermal behaviour of the mould.

Regarding the external temperatures (T2 and T3), the agreement between experimental measurements and numerical predictions is nearly perfect, further confirming the accuracy of the proposed model. In particular, temperature T2 was consistently higher than T3, with average experimental values of approximately 26 °C and 21 °C, respectively. The corresponding numerical discrepancies remained below 4 °C for both measurement locations.

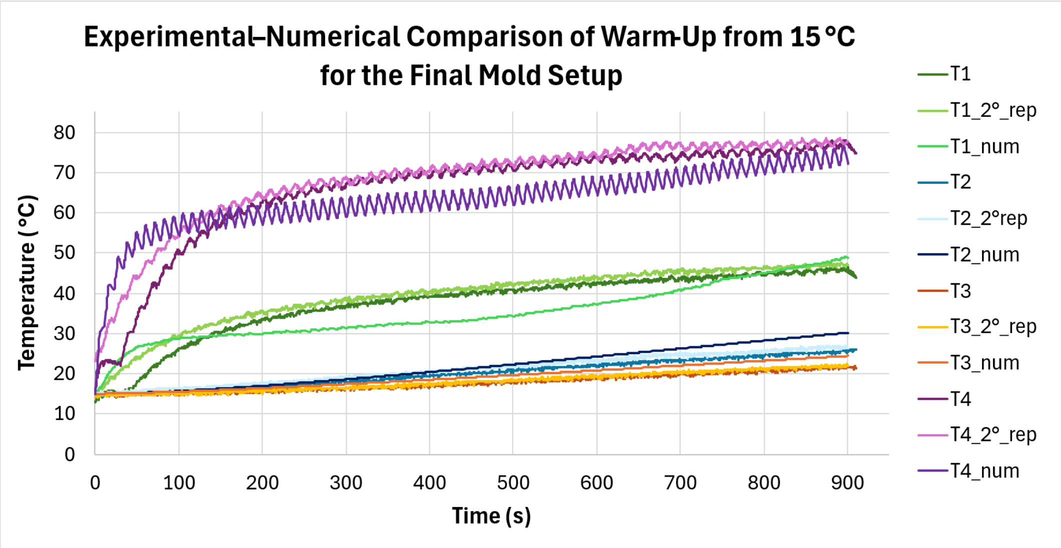

Fig. 7. Experimental–numerical comparison of temperature transients measured by thermocouples.

Conclusion

This work presented the design, experimental characterization, and numerical modelling of a hybrid mould architecture combining polymeric support plates with additively manufactured steel inserts for micro-injection moulding. The experimental campaign demonstrated the mechanical robustness of the polymer-based mould components and enabled the acquisition of reliable thermal transient data under uncooled operating conditions.

A three-dimensional transient numerical model was developed in COMSOL Multiphysics and calibrated using dedicated experimental measurements. Particular emphasis was placed on the identification of the thermal boundary conditions at the injection and extraction interfaces, whose influence was found to be dominant in governing the temperature evolution of the small-scale inserts. Based on the calibration results, an injection-side heat transfer coefficient of 600 W/m²K was selected during the active moulding stages (filling and holding), reduced to 50 W/m²K during passive phases, while the extraction side was modelled using a time-dependent coefficient decreasing from 3000 to 500 W/m²K. The comparison between numerical predictions and experimental results during real moulding cycles confirmed the capability of the model to capture both the rapid heating of the fixed insert and the slower response of the movable side, providing a reliable description of the thermal behaviour of the hybrid mould system. Despite the geometric simplifications adopted to reduce computational cost, the calibrated parameters allowed the model to accurately reproduce the measured thermal transients, with deviations generally within 10% under calibration conditions.

Overall, the proposed experimental-numerical methodology provides an effective tool for the prediction and control of mould thermal behaviour in micro-injection moulding, reducing the need for extensive trial-and-error testing and supporting early-stage tooling design. The results highlight the relevance of accurate boundary-condition calibration when modelling hybrid and thermally insulated mould architectures, where heat exchange with the machine components plays a critical role. Although the presented approach was developed for micro-injection moulding, where reduced mass and thermal inertia amplify heat-transfer effects, the methodology can be extended to other unconventional mould configurations requiring reliable thermal modelling and parameter identification.

Fundings

This work was supported by the European Union under the Italian National Recovery and Resilience Plan (NRRP) of NextGenerationEU, partnership on "Next generation of sustainable and highly efficient moulding processes" Italian Projects of Significant National Interest (PRIN) PNRR 2022 grant n. P2022ZE23N. This work was also supported by PNRR–M4C2INV1.5, NextGenerationEU - Avviso 3277/2021 -ECS_00000033-ECOSISTER-spk 3 and PR-FESR 2021-2027 - Priorità 1 - obiettivo specific 1.1 - Azione 1.1.2 - Progetto "CUP E17G22001630003-SAFER".

Acknowledgement

The authors would like to thank Mr. Elia Andretto from CNR STIIMA for his support in the technological aspects of the research.

References

[1] H. Fu et al., «Overview of Injection Moulding Technology for Processing Polymers and Their Composites», ES Mater. Manuf., vol. Volume 8 (June 2020), fasc. 20, pp. 3–23, mag. 2020.

[2] C. Van Emburg, H. Chen, S. Pilla, G. Li, e M. Carbajales-Dale, «Quantifying energy consumption variability in injection moulding: A meta-regression analysis», Resour. Conserv. Recycl., vol. 227, p. 108730, mar. 2026, doi: 10.1016/j.resconrec.2025.108730.

[3] Y. Kanematsu, H. Noguchi, T. Semba, H. Yano, e Y. Kikuchi, «Life Cycle Assessment of Automobile Parts Made of Cellulose Nanofiber-Reinforced Bio-Polyethylene Using the Pulp Direct Kneading Method», 8 ottobre 2025, ChemRxiv. doi: 10.26434/chemrxiv-2025-qhs18.

[4] T. M. T. Uyen, P. S. Minh, e B. C. Thanh, «Application of Cooling Layer and Thin Thickness Between Coolant and Cavity for Mould Temperature Control and Improving Filling Ability of Thin-Wall Injection Moulding Product», Polymers, vol. 17, fasc. 19, p. 2658, set. 2025, doi: 10.3390/polym17192658.

[5] D. Masato, D. Kazmer, e A. Gruber, «Meta-analysis of thermal contact resistance in injection moulding: A comprehensive literature review and multivariate modeling», Polym. Eng. Sci., vol. 63, fasc. 12, pp. 3923–3937, 2023, doi: 10.1002/pen.26496.

[6] M. Pagac et al., «A Review of Vat Photopolymerization Technology: Materials, Applications, Challenges, and Future Trends of 3D Printing», Polymers, vol. 13, fasc. 4, p. 598, feb. 2021, doi: 10.3390/polym13040598.

[7] J. H. Lee et al., «Quick-Delivery Mould Fabricated via Stereolithography to Enhance Manufacturing Efficiency», Micromachines, vol. 15, fasc. 11, p. 1345, ott. 2024, doi: 10.3390/mi15111345.

[8] T. Hanemann, A. Klein, H. Walter, D. Wilhelm, e S. Antusch, «Evaluation of Material Extrusion Printed PEEK Mould Inserts for Usage in Ceramic Injection Moulding», J. Manuf. Mater. Process., vol. 8, fasc. 4, p. 156, lug. 2024, doi: 10.3390/jmmp8040156.

[9] Y. Lay, R. Roj, M. Bonnet, R. Theiß, e P. Dültgen, «Design and Validation of Additively Manufactured Injection Moulds», 3D Print. Addit. Manuf., vol. 10, fasc. 2, pp. 226–235, apr. 2023, doi: 10.1089/3dp.2021.0132.

[10] H. M. Silva, «A review of the design optimization of conformal cooling channels in injection moulds», Int. J. Adv. Manuf. Technol., vol. 138, fasc. 7, pp. 2653–2671, giu. 2025, doi: 10.1007/s00170-025-15234-2.

[11] D. Chalicheemalapalli Jayasankar, T. Tröster, e T. Marten, «Optimizing Injection Moulding Tool Design with Additive Manufacturing: A Focus on Thermal Performance and Process Efficiency», Materials, vol. 18, fasc. 3, p. 571, gen. 2025, doi: 10.3390/ma18030571.

[12] D. Yao, S.-C. Chen, e B. H. Kim, «Rapid thermal cycling of injection moulds: An overview on technical approaches and applications», Adv. Polym. Technol., vol. 27, fasc. 4, pp. 233–255, 2008, doi: 10.1002/adv.20136.

[13] S.-C. Chen, W.-R. Jong, Y.-J. Chang, J.-A. Chang, J.-C. Cin, «Rapid mould temperature variation for assisting the micro injection of high aspect ratio micro-feature parts using induction heating technology», J. Micromech. Microeng., vol. 16, fasc. 9, pp. 1783–1791, 2006, doi: 10.1088/0960-1317/16/9/005.

[14] Q. Su, N. Zhang, M. D. Gilchrist, «The use of variotherm systems for microinjection moulding», J. Appl. Polym. Sci., vol. 133, p. 42962, 2016, doi: 10.1002/app.42962.

[15] F. De Santis, R. Pantani, «Development of a rapid surface temperature variation system and application to micro-injection moulding», J. Mater. Process. Technol., vol. 237, pp. 1–11, 2016, doi: 10.1016/j.jmatprotec.2016.05.023.

[16] J. Giboz, T. Copponnex, P. Mélé, «Microinjection moulding of thermoplastic polymers: a review», J. Micromech. Microeng., vol. 17, p. R96–R109, 2007, doi: 10.1088/0960-1317/17/6/R02.

[17] K. Oubellaouch, M. Sorgato, e B. Reggiani, «A Two-Step Simulation Approach to Predict Surface Micro-textures Replication in Injection-Moulded Polymeric Parts», in Selected Topics in Manufacturing: Emerging Trends from the Perspective of AITeM's Young Researchers, L. Fratini, L. M. Galantucci, e L. Settineri, A c. di, Cham: Springer Nature Switzerland, 2025, pp. 157–173. doi: 10.1007/978-3-031-99501-9_10.

[18] Giulia Zaniboni, Riccardo Pelaccia, Leonardo Orazi, Rossella Surace, Giovanna Rotella, Vito Basile, Resin moulds to improve thermal energy consumption in injection moulding process, Materials Research Proceedings, Vol. 57, pp 393-400, 2025. DOI: https://doi.org/10.21741/9781644903735-46.

[19] Serratore, Giuseppe, et al. "Life cycle assessment-guided design for sustainable microinjection moulds." Materials Research Proceedings 54 (2025).